
Reaction Dynamics and Charge Transfer in the Scattering of State-Selected Ions on Surfaces

Patricia L. Maazouz

Publication Date

15-04-2004

License

This work is made available under a All Rights Reserved license and should only be used in accordance with that license.

Citation for this work (American Psychological Association 7th edition)

Maazouz, P. L. (2004). *Reaction Dynamics and Charge Transfer in the Scattering of State-Selected Ions on Surfaces* (Version 1). University of Notre Dame. <https://doi.org/10.7274/7h149p30z5r>

This work was downloaded from CurateND, the University of Notre Dame's institutional repository.

For more information about this work, to report or an issue, or to preserve and share your original work, please contact the CurateND team for assistance at curate@nd.edu.

CHAPTER 5

ABSTRACTION REACTION DYNAMICS: $\text{NO}^+(\text{X}^1\Sigma^+)$ + O/Al(111)

5.1. Introduction

The two previous chapters described the detailed reaction dynamics for scattering reactive particles on clean metal surfaces. Another class of fundamentally interesting gas/surface reactions occurs when reactive gases scatter on adsorbate-covered surfaces. For these reactions the incident projectiles require sufficient energy to overcome barriers as incident projectiles react with the adsorbates to form scattered products. Specifically, abstraction reactions may occur when an adsorbate atom is transferred to an incident molecule as the molecule impacts the surface, as described in Section 1.5. These reactions are often assigned to one of two limiting mechanisms: Langmuir-Hinshelwood (LH), where both reagents equilibrate with the surface and Eley-Rideal, where the incident projectile reacts directly with the surface adsorbate.

The majority of abstraction reactions observed to date have been the results of the incident projectile reacting with a hydrogen atom weakly bound to the surface.¹ The strong binding energy of oxygen on aluminum makes O-atom abstraction difficult in the present system. It is commonly accepted that oxygen adsorption on Al(111) is characterized by two adsorption phases: chemisorption and oxide formation.^{2,3} When O_2 dissociatively chemisorbs on initially clean Al(111), the surface becomes dressed

with individual O atoms and (1x1) islands of O atoms, as revealed by scanning tunneling microscopy.³ Although the coverage of isolated chemisorbed atoms does not grow above 0.04 monolayers (ML), the amount of oxygen atoms located within the islands continues to increase with the overall surface coverage.³ Oxide growth commences when the oxygen exposure reaches 60 L (1 L = 10⁻⁶ torr • s), the equivalent of 0.13 ML. Further oxygen uptake leads to a coexistence of the chemisorbed and oxide phases.

In the current experiments the abstraction reaction mechanism is investigated for scattering state-selected NO⁺(X¹Σ⁺) on a clean and adsorbate-covered surface. The yield of NO₂⁻ product ions is measured as a function of the NO⁺(X¹Σ⁺) collision energy and of the amount of oxygen coverage on the surface. In addition, the exit energy of the product ions is measured as a function of the collision energy to help distinguish between a LH or ER abstraction reaction mechanism.

5.2. Experiment

The incident NO⁺(X¹Σ⁺) ions are created in a state-specific manner at the intersection of a supersonic, nitric oxide beam and the frequency-doubled output of a Nd:YAG-pumped dye laser. 2+1 resonance enhanced multiphoton ionization through the H' Σ (J= 0) Rydberg state produces ions in the ground electronic state, NO⁺(X¹Σ⁺), in predominantly the J= 0 vibrational level.⁴ The state-selected ions are extracted, accelerated, mass selected and finally decelerated to 5 - 80 eV before impinging on a clean or oxygen-covered Al(111) surface. The pulsed ion beam typically delivers ~4 x 10⁴ NO⁺ ions per laser shot, corresponding to an exposure rate of 10⁻⁵ L per h. Thus, it is reasonable to assume that the surface coverage is not significantly modified by the impinging NO⁺ ions during the experiment. The chamber

pressure stays below 2×10^{-10} torr when the ion source is running. Surface cleaning comprises several cycles of Ar^+ sputtering (1000 eV, $6 \mu\text{A}$ ion beam directed 60° from the surface normal; $T_s = 300$ K) followed by annealing to 775 K. The cleaning cycles are repeated until contaminant peaks (mainly oxygen and carbon) are absent from the AES spectra, and the LEED pattern shows sharp spots with a low background. Before introducing the NO^+ beam, the surface is dosed with high-purity molecular oxygen through a leak valve. During the dose, the H_2O partial pressure remains less than 1% of the oxygen partial pressure as determined by QMS measurements. Typical doses require 1×10^{-7} torr O_2 for periods up to 40 minutes. The surface temperature is fixed at 300 K through both dosing and scattering phases of the experiment.

The incident and scattered ions are monitored with the ion-imaging detector described in Section 2.5 that was specifically designed to afford mass-to-charge, angle-, and velocity-resolution with near single-ion detection efficiency.⁵ An experiment involves monitoring the relative yield, at a desired product mass, as a function of the NO^+ collision energy and the oxygen dose applied to Al(111) prior to scattering. Background levels were determined by collecting product ions with the surface moved out of the way or by scattering from a clean surface. In both cases, less than one false ion count was registered for every 5×10^8 NO^+ ions incident on the surface.

5.3. Results and Discussion

When state-selected NO^+ ions scatter from the O/Al(111) surface, NO^+ , NO^- , NO_2^- , and O^- are all observed in the experiment. The detection of NO_2^- represents the first evidence that incident molecular ions can directly abstract oxygen atoms from a surface; hence, this discussion focuses exclusively on the mechanism responsible for NO_2^- production. Figure 5.1 shows the dependence of the NO_2^- yield on oxygen exposure

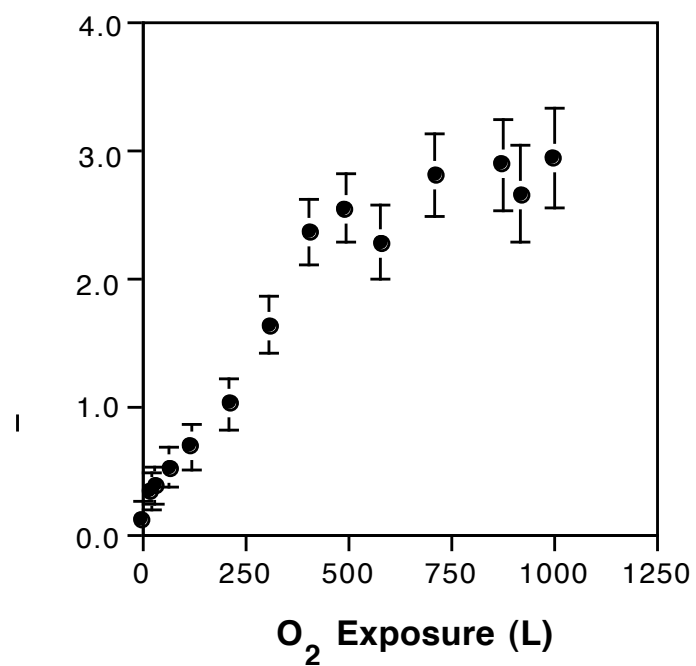


Figure 5.1. Relative yield of scattered NO_2^- as a function of oxygen exposure for NO^+ incident at 40 eV collision energy.

for NO^+ incident with 40 eV collision energy. At zero oxygen exposure, the NO_2^- yield vanishes within the error bars. A linear increase is observed for doses ranging from 0 – 500 L, followed by a more gradual increase for doses up to 1000 L. Because the NO_2^- yield scales with the total coverage of oxygen rather than the coverage of any particular oxygen species on the surface, the abstraction probability appears to be relatively insensitive to the oxygen chemisorption site.

The survival probability of NO^+ incident on O/Al(111) at 40 eV collision energy is approximately 10^{-7} . Such a low measured value indicates that NO^+ is efficiently neutralized on the inbound trajectory prior to surface impact. Only the ground electronic state, $\text{NO}(X^2\Pi)$, can be filled by resonant electron capture from the valence band of aluminum or its oxide. Although electron attachment to form $\text{NO}^-(X^3\Pi^-)$ can occur close to the surface, its efficiency should be low, because the electron affinity of NO (0.026 eV) is small compared with the workfunction (≥ 4.3 eV). This argument is confirmed by the low yield ($<10^{-7}$) of scattered NO^- in the system. Consequently, most of the projectiles impacting the surface are expected to be neutral $\text{NO}(X^2\Pi)$ molecules.

Figure 5.2 presents the NO_2^- yield as a function of $\text{NO}^+(X^1\Sigma^+)$ collision energy for a surface dosed with 750 L O_2 . The NO_2^- yield exhibits a threshold energy of 9 ± 1 eV, above which the yield increases linearly with NO^+ translational energy. Potential mechanisms for NO_2^- formation include (i) sputtering, (ii) collision-induced recombination, (iii) collision-induced desorption followed by gas-phase association, and atom abstraction by either a (iv) Langmuir-Hinshelwood or (v) Eley-Rideal mechanism. The following discussion will address the feasibility of each mechanism. (i) Sputtering of NO_2 contaminants on the surface is unlikely, because NO_2 dissociates completely on Al(111) and does not adsorb on Al_2O_3 at room temperature.^{6,7} (ii) The collisional deposition of energy by an incident projectile may, in principle, induce the recombinative desorption of two or more adsorbates. However, NO and O_2 do not exist as molecular adsorbates on the surface^{7,8} and the three-atom recombination involving one adsorbed

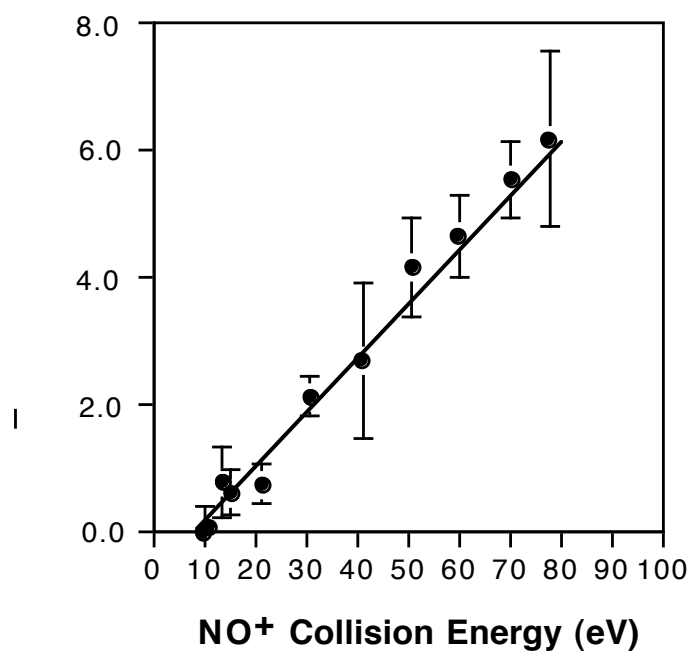


Figure 5.2. The collision-energy dependence to NO_2^- emergence. The Al(111) surface was dosed with 750 L O_2 prior to NO^+ scattering. The straight line is drawn to guide the eye.

nitrogen and two adsorbed oxygen atoms is energetically and sterically implausible. (iii) Kang attributed the formation of a scattered complex, CsX^+ , where Cs^+ is the incident projectile and X is an adsorbate, to a two-step mechanism: collision-induced desorption of X followed by gas-phase association in which Cs^+ and X are united by ion-dipole interactions.⁹ If this were the operative mechanism in the present study, i.e., the ejected NO-O^- molecule is formed by gas-phase association of scattered NO and sputtered O^- , then the threshold for NO_2^- emergence would be greater than or equal to the threshold for sputtered O^- . Anion emission experiments for Na^+ incident on O/Al reveal a 50 eV threshold for O^- sputtering.¹⁰ This is much higher than the 9 eV threshold observed for NO_2^- emergence; therefore, the ion-dipole association mechanism cannot be operative. (iv) The abstraction of an adsorbed O atom by incident NO can occur by either LH or ER mechanisms. In an LH mechanism, the incident NO would thermally accommodate on the surface, diffuse to a chemisorbed oxygen site, react, and desorb as NO_2 . However, the velocity distribution of scattered NO_2^- products is nonthermal and cannot be described by a Maxwell-Boltzmann distribution at the surface temperature (300K). Moreover, the mean translational energy of NO_2^- increases with NO^+ collision energy (see Fig. 5.3). The data indicate that neither the incident NO molecule nor the scattered NO_2^- product resides on the surface long enough to become thermally accommodated. (v) Instead, it is proposed that NO_2^- is formed by a three-step mechanism: incident NO^+ is neutralized close to the surface, nascent NO directly impacts an adsorbed oxygen atom, and O^- is abstracted by NO to form NO_2^- via an ER mechanism. Within the ER mechanism, the NO_2^- product retains “memory” of the incident NO^+ velocity.

The energetics of the proposed Eley-Rideal mechanism are estimated from published thermodynamic data. Neutralization of incident NO^+ creates vibrationally excited $\text{NO}(X^2\Pi)$ and a hole in the valence band that rapidly delocalizes. Estimates of the Franck-Condon overlap between $\text{NO}^+(X^1\Sigma^+)$ and $\text{NO}(X^2\Pi)$ suggest that 0–2 eV of

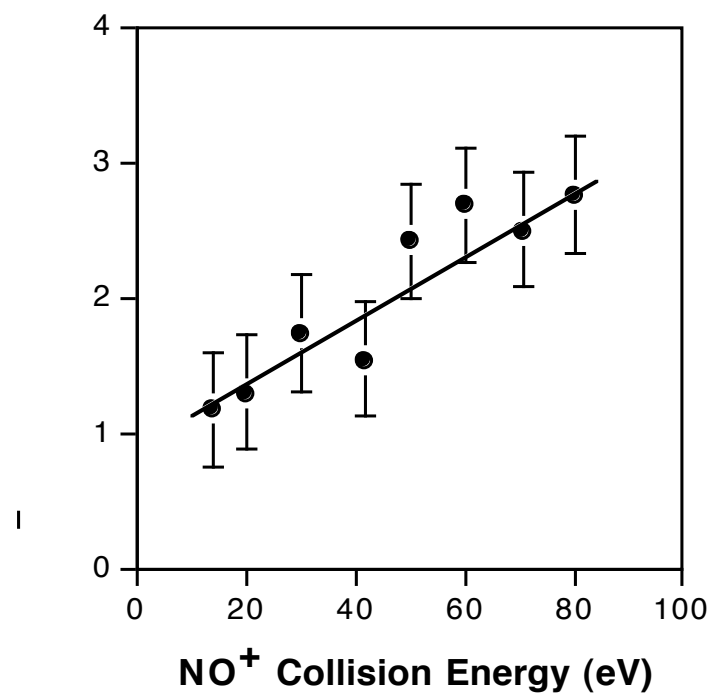


Figure 5.3. Mean translational energy of scattered NO_2^- versus the collision energy of incident NO^+ . The Al(111) surface was dosed with 750 L O_2 . The straight line is drawn to guide the eye.

vibrational energy may be deposited into the nascent NO molecule. *Ab initio* calculations modeling 0.25 ML of oxygen on Al(111) predict that each chemisorbed O atom is bound to the surface by 7.9 eV.¹¹ Theory indicates that oxygen resides on the surface with a -1 rather than a -2 charge, because the adsorbed O atom is not completely coordinated with aluminum ions, as it is in bulk Al_2O_3 . The energy required to remove a chemisorbed O atom from Al(111) and generate an O^- ion in the vacuum is 10.7 eV. The dissociation energy corresponding to $\text{NO}_2^- \rightarrow \text{NO} + \text{O}^-$ is 3.9 eV, as calculated from the 3.1 eV¹² dissociation energy of NO_2 and the electron affinities of O (1.46 eV) and NO_2 (2.27 eV).¹³ Consequently, the observed reaction, $\text{NO} + \text{O}^-/\text{Al} \rightarrow \text{NO}_2^- + \text{Al}$ is endoergic by 6.8 eV, if neutralization of NO^+ exclusively populates $\text{NO}(X^2\Sigma, \Omega = 0)$. To the extent that NO is vibrationally excited after NO^+ is neutralized, the energetic requirements for NO_2^- production will be reduced to ~ 4.8 eV. At threshold, the collision energy (9 eV) minus the sum of the reaction endoergicity and the product kinetic energy (1.1 eV from Fig. 5.3), represents the energy (1 – 3 eV) dissipated by the surface and/or deposited as internal energy into NO_2^- . Although depositing 10%–30% of the incident energy into lattice vibrations seems small, it should be noted that at the reaction threshold, only a limited set of trajectories successfully lead to reaction. Successful trajectories necessarily involve impact parameters and bond orientations ideal for efficient activation of the reaction and correspondingly inefficient energy dissipation to the surface. At higher collision energies, trajectories with varying energy deposition will contribute to the reaction probability. The slope of the line drawn in Fig. 5.3 indicates that $(2.3 \pm 1.0)\%$ of the NO^+ collision energy appears as translational energy in the NO_2^- product. NO_2^- emergence involves the deceleration of the scattered anion as it escapes from the attractive electrostatic potential of the surface. A prior study on a similar system (NO^+ on GaAs) showed that the charge transfer product, NO^- , scatters with only 6% of the NO^+ collision energy.¹⁴ With the masses of aluminum and oxygen being less than those of gallium and arsenic, and with the mass

of NO_2 being greater than that of NO , kinematic arguments correctly predict that the present system should exhibit a greater degree of mechanical energy transfer to the surface than that seen for $\text{NO}^+/\text{GaAs}(110)$.

The abstraction of an O atom from $\text{O}/\text{Al}(111)$ is expected to have a low probability, because the reaction with NO is endothermic by 6.8 eV. However, the recorded relative yield of NO_2^- may be low for the following reasons. The ion-imaging detector measures only the fraction of product ions that scatter into the detector's solid angle of collection. It is estimated that less than 10% of the NO_2^- ions emerging from the surface are directed into the detector's active area. Furthermore, various molecular processes may reduce the amount of detected signal. NO_2^- may transfer an electron into the substrate's conduction band before the molecule escapes into the vacuum. Additionally, during the 5 - 15 μs flight time from the surface to the detector, NO_2^- may undergo autodetachment or unimolecular dissociation if its internal energy exceeds 2.27 eV or 3.92 eV, respectively.¹⁵ Consequently, the reported NO_2^- relative yield underestimates the probability of NO_2^- formation at the surface.

5.4. Summary

These experiments represent the first report of hyperthermal energy, molecular ions abstracting adsorbed oxygen atoms. The velocity distribution of scattered NO_2^- products provides clear evidence for a direct, Eley-Rideal reaction. Nitric oxide abstracts O atoms predominantly from islands of chemisorbed oxygen/oxide species. The observed 9 eV threshold is consistent with thermodynamic estimates of the reaction energetics.

5.5 References

- ¹ C. T. Rettner, *Physical Review Letters* **69** (2), 383 (1992); C. T. Rettner, *Journal of Chemical Physics* **101** (2), 1529 (1994); M. R. Morris, D. E. Riederer, B. E. Winger, R. G. Cooks, T. Ast, and C. E. D. Chidsey, *International Journal of Mass Spectrometry and Ion Processes* **122**, 181 (1992); S. A. Buntin, *Journal of Chemical Physics* **108** (4), 1601 (1998).
- ² I. P. Batra and L. Kleinman, *Journal of Electron Spectroscopy and Related Phenomena* **33** (3), 175 (1984).
- ³ H. Brune, J. Wintterlin, J. Trost, G. Ertl, J. Wiechers, and R. J. Behm, *Journal of Chemical Physics* **99** (3), 2128 (1993).
- ⁴ Franck-Condon overlap between the H¹P(n = 0) Rydberg state and the X1S⁺ ion state predicts a strong propensity for D_n = 0 transitions in the ionization step. Furthermore, there is no evidence for autoionization or strong mixing within the ionization continuum at these photon energies.
- ⁵ D. Corr and D. C. Jacobs, *Review of Scientific Instruments* **63** (3), 1969 (1992); M. Maazouz, J. R. Morris, and D. C. Jacobs, *Ion Imaging in Surface Scattering*. (American Chemical Society, Washington, D.C., 2001).
- ⁶ H. Schlienz, M. Beckendorf, U. J. Katter, T. Risse, and H. J. Freund, *Physical Review Letters* **74** (5), 761 (1995).
- ⁷ T. J. Chuang, R. Schwarzwald, and A. Modl, *Journal of Vacuum Science & Technology a-Vacuum Surfaces and Films* **9** (3), 1719 (1991).
- ⁸ A. Hoffman, T. Maniv, and M. Folman, *Surface Science* **183** (3), 484 (1987).
- ⁹ M. C. Yang, C. H. Hwang, and H. Kang, *Journal of Chemical Physics* **107** (7), 2611 (1997).
- ¹⁰ J. C. Tucek and R. L. Champion, *Surface Science* **382** (1-3), 137 (1997).
- ¹¹ G. Wahnstrom, A. B. Lee, and J. Stromquist, *Journal of Chemical Physics* **105** (1), 326 (1996); J. Jacobsen, B. Hammer, K. W. Jacobsen, and J. K. Norskov, *Physical Review B* **52** (20), 14954 (1995).
- ¹² R. Jost, J. Nygard, A. Pasinski, and A. Delon, *Journal of Chemical Physics* **105** (3), 1287 (1996).
- ¹³ *CRC Handbook of Chemistry and Physics*, edited by D. R. Lide (CRC Press, New York, 1999).
- ¹⁴ J. S. Martin, J. N. Greeley, J. R. Morris, B. T. Feranchak, and D. C. Jacobs, *Journal of Chemical Physics* **100** (9), 6791 (1994).

¹⁵ B. A. Huber, P. C. Cosby, J. R. Peterson, and J. T. Moseley, *Journal of Chemical Physics* **66** (10), 4520 (1977); E. Andersen and J. Simons, *Journal of Chemical Physics* **66** (6), 2427 (1977).